Shift of the Special Pair Redox Potential: Electrostatic Energy Computations of Mutants of the Reaction Center from *Rhodobacter sphaeroides*[†]

I. Muegge,[‡,§] J. Apostolakis,[‡,||] U. Ermler,[⊥] G. Fritzsch,[⊥] W. Lubitz,[∇] and E. W. Knapp*,[‡]

*Freie Universität Berlin, Fachbereich Chemie, Institut für Kristallographie, Takustrasse 6, D-14195 Berlin, Germany,
Max-Planck-Institut für Biophysik, Abteilung Molekulare Membran-biologie, Heinrich-Hoffmann-Strasse 7,
D-60528 Frankfurt, Germany, Technische Universität Berlin, Max-Volmer-Institut, Strasse des 17. Juni 135,
D-10623 Berlin, Germany, University of Southern California, Department of Chemistry, Los Angeles, California 90089-1062,
and Biochemisches Institut, Universität Zürich, Winterthurer Strasse 190, CH-8057 Zürich, Schweiz*

Received September 15, 1995; Revised Manuscript Received March 28, 1996[⊗]

ABSTRACT: Shifts of the special pair redox potential of the photosynthetic reaction center of *Rhodobacter sphaeroides* are considered for several point mutations [Lin, X., Murchison, H. A., Nagarijan, V., Parson, W. W., Allen, J. P., & Williams, J. C. (1994) *Proc. Natl. Acad. Sci. U.S.A. 91,* 10265−10269] in the neighborhood of the special pair. The shifts are calculated from electrostatic energies by solving Poisson's equation for energy-minimized structures of the reaction center. Different conditions for the evaluation of the electrostatic energy are probed. To test the influence of the hydrogen bonding at the acetyl groups of the special pair, the orientation and torsion potential of the acetyl groups are varied. The calculated shifts of the midpoint potential of double and triple mutants can approximately be obtained from the corresponding shifts of the single point mutations. The calculated shifts agree with the measured values for all single and double mutants considered. However, a clear decision between different acetyl group conformations was only possible for the mutants HF(L168) and HF(L168) + LH(L131) where the calculated shifts of the redox potential agree with experiments only if the acetyl oxygen atom at D_M points toward the Mg^{2+} ion of D_L. This is corroborated by computations of the interaction energy of the acetyl group at D_M, which adopts a lower value in the wild-type reaction center if its oxygen atom is bonded to the Mg^{2+} ion of D_L.

The primary charge separation events of photosynthesis take place in the so-called reaction center (RC).[1] Much progress has been made in the understanding of the function of photosynthetic RC's, since the first three-dimensional crystal structure of the RC of the purple photosynthetic bacterium from *Rhodopseudomonas (Rps.) viridis* became available (Deisenhofer et al., 1984, 1985). Shortly afterward the crystal structure of a second RC, from *Rhodobacter (Rb.) sphaeroides*, was determined with an initial resolution of 3.7 Å (Chang et al., 1986) and 2.8 Å (Allen et al., 1987). Recently the structure of *Rb. sphaeroides* was obtained from a trigonal crystal form with a better resolution of 2.65 Å (Ermler et al., 1994), providing a more detailed description of the RC of *Rb. sphaeroides*. This shows that the structures of *Rps. viridis* and *Rb. sphaeroides* RC's exhibit only minor

differences and in particular the overall cofactor arrangement is conserved. Crystal structures of several mutants of *Rb. sphaeroides* are now also available (Chirino et al., 1994). Those structures are not drastically different from that of the wild-type.

The RC of *Rb. sphaeroides* contains the following cofactors: four bacteriochlorophyll a (BChl) (Figure 1), two of them (D_L, D_M) forming the special pair (D), two bacteriopheophytin a (BPh) (Φ_A,Φ_B), two ubiquinones UQ-10, (Q_A, Q_B), one non-heme Fe^{2+}, and one carotenoid. The nomenclature proposed by Hoff (1988) and Deisenhofer and Michel (1991) is used. The chromophores are arranged in two branches, A and B, which are related to each other by an approximate C_2 rotation symmetry (Deisenhofer et al., 1985; Michel et al., 1986; Allen et al., 1987). Only one of the two branches (A) is active. It conducts an electron from the singlet excited donor (D) in about 3.5 ps (Woodbury et al., 1985; Breton et al., 1988) to Φ_A, the pheophytin of the active branch. This initial electron transfer step is supported by the accessory BChl (B_A) which is discussed to serve as a first intermediate electron acceptor (Zinth & Kaiser, 1993; Kirmaier & Holten, 1993). The details of the initial electron transfer are still a matter of debate (Creighton et al., 1988; Scherer & Fischer, 1989a; Bixon et al., 1991, 1992). In another 200 ps (Kirmaier & Holten, 1987) the electron is transferred to the primary Q_A and finally within about 100 μs to the secondary quinone Q_B. The charge-separated state is subsequently stabilized by neutralizing the positive charge at the special pair with an electron transferred from a soluble cytochrome c_2. After reduction of the quinone Q_B (Q_A) the forward electron transfer is blocked such that the transfer

* To whom correspondence should be addressed at FU Berlin, Fachbereich Chemie, Institut für Kristallographie, Takustrasse 6, D-14195 Berlin, Germany.

‡ Freie Universität, Berlin.

§ Present address: University of Southern California, Los Angeles, CA.

|| Present address: Biochemisches Institut, Universität Zürich, Switzerland.

⊥ Max-Planck-Institut für Biophysik, Frankfurt.

∇ Technische Universität, Berlin.

[1] Abbreviations: RC, reaction center; *Rps., Rhodopseudomonas*; *Rb., Rhodobacter*; D, special pair; BChl, bacteriochlorophyll a; Bph, bacteriopheophytin a; UQ-10, ubiquinone; Q, quinone; E_M, midpoint potential; mut, mutant; WT, wild-type; s, strong; w, weak.
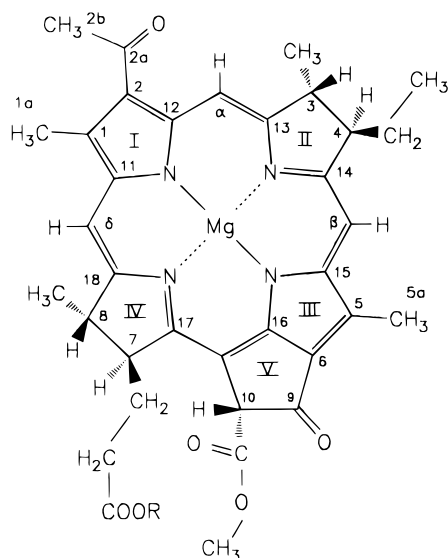
FIGURE 1: Molecular structure of BChl a (R = phytyl chain) with atom numbering scheme. The carbonyl oxygen atoms at ring I and V can act as hydrogen bond acceptors.

back to the special pair may also occur from the Q_A (Φ_A).

To understand the role of the protein environment on the function of the cofactors, specific amino acid residues have been exchanged by site-directed mutagenesis (Williams et al., 1992; Nagarajan et al., 1993; Murchison et al., 1993; Lin et al., 1994a,b). Several mutations in RC's of *Rb. sphaeroides* have been designed to modify the environment of the special pair (see Table 1). By replacing amino acids, the electrostatic environment and possibly also the hydrogen bond pattern of the special pair are changed. As a consequence the electrochemical midpoint potential (E_M)

$$E_M = E(D^0) - E(D^+) + \Delta E(H_{electrode}) \qquad (1)$$

accounting for the free energy difference between the reduced (D^0) and oxidized (D^+) special pair state is shifted (see Table 1). The E_M is measured against the normal hydrogen electrode, which contributes an extra term, $\Delta E(H_{electrode})$.

The E_M of the special pair determines the driving force for the primary process of charge separation as well as charge recombination of D^+ with Φ^-_A, Q^-_A, and Q^-_B. The measured shifts of the E_M correlate well with the changes in the electron transfer rates (Lin et al., 1994a,b). Furthermore the functionally important re-reduction of D^+ by cytochrome c_2 strongly depends on the E_M of the special pair (Lin et al., 1994b).

The mutants of the RC in which amino acids are exchanged in the neighborhood of the special pair demonstrate that the E_M depends strongly on the number and strength of the hydrogen bonds formed with carbonyl oxygen atoms of the special pair (Lin et al., 1994a,b). The hydrogen bonding pattern determines also the orientation of the acetyl groups at the special pair (Figure 1). In the absence of a hydrogen bond it is assumed that the acetyl group adopts an in-plane orientation with respect to the porphyrin plane (Ermler et al., 1994). On the basis of quantum chemical computations it was found that the special pair bands in the optical absorption spectrum undergo a red-shift if the acetyl group of the special pair is rotated from an in-plane to an out-of-plane conformation (Parson & Warshel, 1987; Warshel & Parson, 1987). Recent measurements of low-temperature

optical absorption spectra of mutant RCs of *Rb. sphaeroides* corroborate this result (Mattioli et al., 1995; Rautter et al., 1995).

Since the E_M of a cofactor is sensitive to the protein environment, structural changes induced by mutations can be deduced from a comparison between calculated and measured E_M's. Thereby it should be possible to supply details of mutant structures which differ from the wild-type. One possibility of such changes is the ring I acetyl group at D_M whose orientation of the oxygen atom pointing away from the Mg^{2+} ion of D_L is only slightly favored by the electron density map (Ermler, et al., 1994).

It is now a decade ago that redox potentials in proteins could be calculated successfully (Churg & Warshel, 1986). In the present work the shift of the E_M of the special pair of *Rb. sphaeroides* is calculated for eleven different mutants and compared with experimental data. Different conformations of the ring I acetyl group (Figure 1) are probed by varying the corresponding torsion potential and the start conformation. The E_M's are evaluated by solving Poisson's equation using the program DelPhi (Gilson et al., 1985; Klapper et al., 1986; Nicholls et al., 1991).

METHODS

Use of the Dielectric Constant for the Computations with DelPhi. The atomic partial charges of the amino acids are taken from CHARMM22 (Brooks et al., 1983). For molecular dynamics simulations CHARMM is typically used with a dielectric constant of $\epsilon = 1$ (Elber & Karplus 1990). Also the water model TIP3P (Jorgensen et al., 1983) used in the present computations was designed for a dielectric constant of unity. To account for effects of atomic polarization these water models have a permanent dipole moment which is closer to the value in ice (2.6 D) than to the value in the gas phase (1.85 D) (Coulson & Eisenberg, 1966). For the TIP3P water model the permanent dipole moment is 2.35 D.

In a conventional treatment with DelPhi for the wild-type RC the crystal structure is used without changes. For mutants with unknown structure the protein structure is generated by modeling and kept as close as possible to the crystal structure. Differently charged states are not energy minimized separately. To account for the lack of atomic and molecular polarizibility a dielectric constant of 4 is normally used within the protein molecule (Gilson et al., 1986; Gunner & Honig, 1991). In the present application of DelPhi all protein structures used are energy minimized. This may contribute to part of the molecular polarization which is due to the reorientation of polar groups. To be consistent with the treatment of the electrostatic interactions in molecular dynamics simulations using the CHARMM force field the dielectric constant within the protein molecule is set here to unity ($\epsilon_p = 1$). As is demonstrated below, larger values of the dielectric constant lead to shifts of the redox potential whose absolute values are too small. The unusually small value of the dielectric constant used in this work may be justified in this case for the following reasons. The shifts of the redox potential considered here are due to changes of the local hydrogen bond interactions for which the CHARMM force field is tuned specifically. On the other hand a continuous dielectric medium has problems to account properly for dielectric screening on very short distances.

For each protein atom a volume corresponding to its Van der Waals radius is assigned and a spherical probe particle

Table 1: Mutations near the Special Pair of *Rb. sphaeroides* and Their Measured Change of Midpoint Potential ΔE_M

no.	mutant	ΔE_M (mV)	reference	remarks
0	WT	0^a		wild-type
1	FH(M197)	$+125 \pm 10$	b	forms H-bond with ring I acetyl oxygen of D_M
2	HF(L168)	-95 ± 10	b,c	loss of H-bond with ring I acetyl oxygen of D_L
3	LH(M160)	$+60 \pm 10$	b,d	forms H-bond with ring V keto oxygen of D_M
4	LH(L131)	$+80 \pm 10$	b,d	forms H-bond with ring V keto oxygen of D_L
5	FH(M197) + HF(L168)	$+40 \pm 10$	b	see single point mutations 1 and 2
6	FH(M197) + LH(M160)	$+195 \pm 10$	b	see single point mutations 1 and 3
7	FH(M197) + LH(L131)	$+205 \pm 10$	b	see single point mutations 1 and 4
8	HF(L168) + LH(M160)	$+20 \pm 10$	b	see single point mutations 2 and 3
9	HF(L168) + LH(L131)	-20 ± 10	b	see single point mutations 2 and 4
10	LH(L131) + LH(M160)	$+130 \pm 10$	b	see single point mutations 3 and 4
11	FH(M197) + LH(L131) + LH(M160)	$+260 \pm 10$	b	see single point mutations 1, 3, and 4

[a] The reference value of WT is $E_M = 500 \pm 5$ mV (Williams et al., 1992; Nagarajan et al., 1993; Lin et al., 1994a,b). [b] Lin et al. (1994a,b). [c] Murchison et al. (1993). [d] Williams et al. (1992).

of 1.4 Å radius defines the protein−solvent surface boundary. Large enough cavities in the protein which are not occupied by crystalline water molecules have a dielectric constant with the same value as in the solvent, $\epsilon_w = 80$. A physiological ionic strength of 0.145 M/L with a 2 Å ion exclusion layer is used.

The membrane regime is defined by a layer of 30 Å thickness. The RC is centered in this membrane with the C_2 symmetry axis of the RC orthogonal to the membrane plane. Though the membrane is not modeled by explicit atoms, the dielectric constant in this regime is also set to unity ($\epsilon_m = 1$), since DelPhi allows only two different values of the dielectric constant. However, test calculations with other values for the dielectric constant ($\epsilon_m = \epsilon_p = 2$, $\epsilon_w = 80$; $\epsilon_m = \epsilon_p = 4$, $\epsilon_w = 80$; $\epsilon_m = \epsilon_w = 80$, $\epsilon_p = 4$) are also performed.

Generation of the Mutant Structures. The mutant structures are derived from the wild-type crystal structure of the RC by elementary modeling techniques. For the mutants FH, HF, and LH first all side-chain atoms except the carbon atoms C_β and C_τ are removed. Then the corresponding side-chain ring atoms are added in idealized geometry such that the orientation of the ring plane is retained for the mutants FH and HF. Care is taken to ensure that the residues mutated to histidine can form the corresponding hydrogen bonds. These are a hydrogen bond with the acetyl oxygen atom at D_M for FH(M197) and a hydrogen bond with the keto oxygen atom at D_M [D_L] for LH(M160) [LH(L131)].

Computational Conditions for Applications with DelPhi. Before the calculations with DelPhi can be started, the following steps of preparation of the coordinates from the crystal structure of *Rb. sphaeroides* are made and described in more detail below: hydrogen atoms are added (point 1); specific constraints are used (point 2); the torsion potentials of the acetyl groups are defined (point 3); water molecules are added (point 4); the whole RC is energy minimized (point 5); the atomic partial charges are defined (point 6); conditions for the solution of Poisson's equation are set (point 7).

(1) Hydrogen atoms are added using the program CHARMM (Brooks et al., 1983). The cofactors BChl and BPh are modeled in an all-hydrogen atom representation. For the amino acid residues only hydrogen atoms in polar bonds are added. All other hydrogen atoms are represented by corresponding extended atom types.

(2) All atoms of residues which are completely outside of a sphere of radius 18.5 Å centered at the geometrical midpoint of the residues L168 and M197 are spatially fixed.
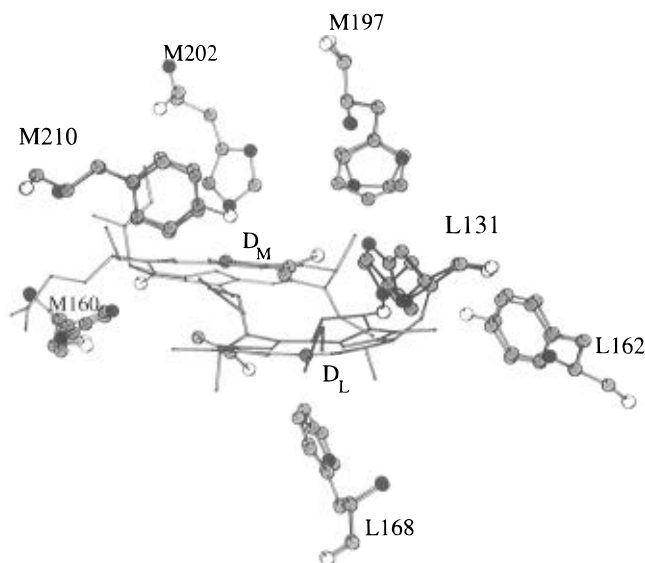

FIGURE 2: Special pair of the RC *Rb. sphaeroides* with mutated residues. Energy-minimized structures of the wild-type and mutated residues at the special pair are depicted together with a fixed special pair structure using the actual crystal structure by Ermler et al. (1994). The oxygen atoms are represented by open, the nitrogen atoms by black and the carbon atoms by gray circles. The cytochrome c_2 is located at the side of the residue L162. The active branch (A) of the RC is situated at the side of the residues M202 and M197.

This reference point is close to the geometrical center of the residues whose mutations are considered (Figure 2). To keep the geometry of the special pair close to the crystal structure all non-hydrogen atoms of the special pair are fixed. The only exceptions are the atoms of the ring I acetyl groups of D_L and D_M. They are kept mobile with respect to the torsion angle. This allows for rearrangements of the acetyl group to form or break hydrogen bonds.

(3) The torsion potential used for the acetyl group is

$$V_{torsion}(\gamma) = k(1 - \cos 2\gamma) \qquad (2)$$

It possesses minima for the orientations $\gamma = 0, \pi$ in the corresponding porphyrin plane. Two values of the interaction parameter k are used. The original value of the force constant in CHARMM, $k_s = 2$ kcal/mol (s = strong) allows for minor deviations from the in-plane conformation of the acetyl group only. Alternatively a smaller value, $k_w = 0.5$ kcal/mol (w = weak), is used, which allows also for out-of-plane orientations of the acetyl group. Note that sterical

hindrance by unfavorable Van der Waals interactions is not contained in the torsion potential. This interaction can also prevent a complete reorientation of the acetyl groups. Corresponding data are referred to by subscripts s and w, respectively.

(4) To restrict conformational changes to a minimum, cavities inside the sphere of 18.5 Å radius are filled with water molecules by using an overlay technique (Knapp & Nilsson, 1990; Wade et al., 1991) where water molecules are added if the water oxygen to protein heavy atom distance is larger than 2.8 Å. According to our experience this distance criterion is not severe, allowing water molecules to be introduced only into cavities which are large enough. In this way 203 water molecules were added to the 165 water molecules already present in the X-ray structure within the sphere of 18.5 Å radius. The employed water model is a variant of TIP3P (Jorgensen et al., 1983; Blumhagen et al., 1995).

(5) The whole protein−water system of the wild-type RC consisting of 10 125 atoms is energy minimized with CHARMM using the constraints described in points 2−4. The energy minimization is repeated for each mutant, for different orientations of the ring I acetyl group at D_M and the two charge states of the special pair (D^0, D^+). The root mean square deviations (rmsd) between different energy-minimized structures are small. For the wild-type RC and the mutant FH(M197) both in the reduced special pair state the rmsd value is 0.042 Å for all non-hydrogen atoms. For the special pair atoms excluding the acetyl group atoms the corresponding rmsd values are somewhat larger, namely, 0.139 Å for $D_M{}^0$ and 0.126 Å for $D_L{}^0$.

Polar and charged residues which are spatially close to the mutated residue M197 can have much larger rmsd values. The largest rmsd values are found for asparagine M199 where the average rmsd value is 0.54 Å, and the side-chain oxygen atom has an rsmd value of 1.70 Å. Only few other residues have average rmsd values larger than 0.3 Å. The rmsd values of other mutants are similar. The rmsd values between different redox states of the same RC are smaller. For the wild-type RC the rmsd values are 0.012 Å for all atoms, 0.029 Å for D_M, and 0.025 Å for D_L. Here the largest rmsd values are observed for residue aspartate L155, where the average value is 0.24 Å.

Alternatively structures from "simulated annealing" (Kirkpatrick et al., 1983) of the different protein−water systems are also used. The following protocol for the annealing is used. The relevant part of the RC defined in point 2 is coupled to a heat bath with a temperature of 400 K, and its dynamics are simulated for 5 ps. Next, the heat bath temperature is set to 0 K and the dynamics simulation is continued for another 5 ps. Finally the complete RC structure is energy minimized.

(6) The atomic partial charges of the amino acid residues are taken from the parameter set of CHARMM22. The charge distribution of the cofactors are obtained from quantum chemical computations using the convention of Mulliken (1955) to assign atomic partial charges. The atomic partial charges at the two ubiquinones have been calculated with Gaussian 92 (Frisch et al., 1992). The charges of the BChl's, BPh's, the carotenoid, and the detergent molecule (LDAO) were calculated with a semiempirical INDO SCF-MO method (Pople & Beveridge, 1970; Dewar et al., 1968). For the neutral and positively charged special pair the charge

distributions are taken from computations of Plato et al. (1986, 1991) which were based on the crystal structure of *Rb. sphaeroides* of Allen et al. (1987). For the oxidized special pair $\Delta q_M = 0.28$ ($\Delta q_L = 0.72$) of the unit positive charge is localized at D_M (D_L). The computed ratio of charges at the special pair BChl's of the wild-type RC Q(WT) $= \Delta q_L/\Delta q_M = 2.57$ correlates well with the corresponding ratio of the measured spin density S(WT) $= 2.09$ (Lendzian et al., 1993). The atomic partial charges of the reduced (oxidized) special pair are for the three most relevant atoms: the magnesium, the oxygen, and the carbon atoms of the acetyl group at the BChl D_M +0.396 (+0.414), −0.350 (−0.353), and +0.307 (+0.306), and at the BChl D_L +0.395 (+0.429), −0.339 (−0.325), and −0.326 (−0.325). The atomic partial charges of the other cofactors, the two accessory BChl's, BPh's, the carotenoid, and the detergent molecule (LDAO) are adapted from the charges of the corresponding cofactors in *Rps. viridis* as calculated by Scherer and Fischer (1989b) with a semiempirical INDO SCF-MO method.

(7) The electrostatic potential is obtained by solving Poisson's equation. DelPhi maps the atomic partial charges and the dielectric constant onto a 65^3 point grid and solves Poisson's equation with a finite difference algorithm (Klapper et al., 1986; Gilson et al., 1985). To ensure that the results do not depend on the grid size, a series of focusing calculations are made (Gilson et al., 1987, 1988) centered at the midpoint of the Mg^{2+} ions of the special pair. The initial grid spacing is 2.0 Å, and the final spacing is 0.5 Å.

Evaluation of the Redox Potential. The difference of the electrostatic energy between the neutral (0) and positively (+) charged special pair state is calculated by

$$\Delta G = G(0) - G(+) \tag{3}$$

with

$$G(\alpha) = \sum_i \Phi_i(\alpha) q_i(\alpha) \tag{4}$$

where α denotes the charge of the special pair (0 or +), $q_i(\alpha)$ denotes the atomic partial charge, and $\Phi_i(\alpha)$ denotes the electrostatic potential at atom i due to all atoms of the system which do not belong to the special pair. This expression involves a sum over all atoms of the special pair and refers to a structure which is energy minimized for the corresponding charge state α of the special pair. It does not account for the Born energy of the special pair atoms in the heterogeneous dielectric medium of the protein−water system. Its contribution to ΔE_M has been calculated and is in all cases considered smaller than 10 mV.

Since for each charge state a separate energy minimization of the system is made, the atomic coordinates of the protein environment depend on the charge of the special pair. Hence, Poisson's equation must be solved for each charge state separately to obtain the corresponding electrostatic energies of eqs 3 and 4. The shift of the redox potential ΔE_M is calculated as double difference of the free energy expression 3

$$\Delta\Delta G = \Delta G_{mut} - \Delta G_{WT} \tag{5}$$

According to the Nernst equation

$$\Delta E_{\mathrm{M}} = -\frac{\Delta\Delta G}{nF} \qquad (6)$$

In expression 6, $n = 1$ is the change of elementary charge in the redox reaction and $F = 96\,485$ C/mol is Faraday's constant. The subscript mut refers to one of the mutants listed in Table 1, and the subscript WT refers to the wild-type RC.

RESULTS

Survey of Results. The shifts of the E_{M} of the special pair in *Rb. sphaeroides* are calculated for eleven mutants where the hydrogen bonding pattern to the special pair is changed. These mutants are listed in Table 1 together with the experimental values of ΔE_{M} (Lin et al., 1994). The calculated shifts of the E_{M} evaluated with DelPhi are given in Table 2 for different orientations of the acetyl groups at the special pair and two values of the dielectric constant for the RC ($\epsilon_{\mathrm{p}} = 1$ and $\epsilon_{\mathrm{p}} = 2$).

The structures of the mutant RC's are generated by placing the atoms of the mutated residues at the position of equivalent atoms of the corresponding wild-type residue. The mutated residues are visualized in Figure 2 for energy-minimized mutant structures together with an average special pair structure. It is obvious from this figure that the energy minimization does not change the position of equivalent atoms of different mutants significantly. On average, the differences between the structures of wild-type and mutant RC's are small. The structures of RC's with different orientations of the acetyl group at D_{M} are displayed and explained in Figure 3. This figure also demonstrates structural differences of the acetyl group at D_{M} occurring with different charge states of the special pair. In general these structural differences are small. More details on structural differences between mutant and wild-type RC's and different redox states of the special pair are given in the Methods section under point 5 of the computational conditions.

The largest direct contributions to the calculated shifts of the E_{M} are due to the mutated residue, and only a small fraction is due to the acetyl groups (see Table 4). Nevertheless, the indirect influence of the orientation of the acetyl groups on the shift of E_{M}, which also leads to reorientations of the mutated residues, can be quite large. This is demonstrated in Figure 4 for the acetyl group at D_{M} in the mutant FH(M197), where the shift of the E_{M} exhibits a strong dependence on the orientation of the acetyl group in the mutant RC. The influence of explicit water molecules and different dielectric media on the calculated shift of the E_{M} is demonstrated for the mutant FH(M197) in Table 3. Details on the geometry and energetic of the formation of the hydrogen bond in the mutant FH(M197) are given in Table 5.

Hydrogen Bonding Pattern of the Special Pair. The mutants listed in Table 1 have been designed to add or remove hydrogen bonds at the special pair of the RC from *Rb. sphaeroides* as indicated in the last column of Table 2. The single-point mutation FH(M197) and all double and triple mutants 5, 6, 7, and 11 involving this mutation add a hydrogen bond to the acetyl oxygen atom at D_{M}. In the single-point mutation HF(L168) and the corresponding double mutants 5, 8, and 9 the hydrogen bond formed between the acetyl oxygen atom at D_{L} and H(L168) present in the wild-type RC is removed. In the single point mutant LH(M160) [LH(L131)] and the corresponding double and triple mutants 6, 8, 10, and 11 [7, 9, 10, and 11] the ring V keto oxygen atom of D_{M} (D_{L}) forms an additional hydrogen bond with H(M160) [H(L131)]. The existence or absence of the hydrogen bonds has been confirmed by corresponding changes in FTIR and resonance Raman vibrational spectra (Nabedryk et al., 1993; Mattioli et al., 1994, 1995).

A change in the hydrogen bonding pattern of the special pair has a dramatic influence on the E_{M} values. In all cases considered a carbonyl oxygen atom of the special pair serves as a hydrogen atom acceptor. With the formation (removal) of each hydrogen bond the E_{M} value is up-shifted (down-shifted) by $80-120$ mV. These shifts can be used to probe the change in hydrogen bonding scheme accompanying the considered mutation (Wachtveitl et al., 1993; Mattioli et al., 1995). To investigate these effects the computations of the shift ΔE_{M} are performed for different orientations of the ring I acetyl group of D_{M}.

Crystal Structure and Orientation of the Acetyl Groups. In the RC from *Rps. viridis* (Deisenhofer et al., 1984, 1985) the special pair forms three hydrogen bonds with the RC environment. The special pair in the RC from *Rb. sphaeroides* possesses only one hydrogen bond involving the ring I acetyl oxygen atom of D_{L} and the residue His(L168) (Ermler et al., 1994). The ring I acetyl group of D_{M} has an in-plane orientation, and there is a weak preference in the electron density map that the acetyl oxygen atom points away from the Mg^{2+} ion of D_{L}. In *Rb. sphaeroides* the amino acid residue related by C_2 symmetry to histidine L168 is phenylalanine M197 (tyrosine in *Rps. viridis*), which in contrast to *Rps. viridis* cannot form a hydrogen bond with the acetyl oxygen atom at D_{M}. One major difference of the special pair structure in *Rps. viridis* and *Rb. sphaeroides* is the conformation of ring V of D_{L}. In *Rb. sphaeroides* it is bent in the opposite direction than in *Rps. viridis*, where the ring V keto oxygen atom of D_{L} forms a hydrogen bond with the hydroxyl group of T(L248). In *Rb. sphaeroides* this keto oxygen atom has an unfavorable contact to the side chain of M(L248).

In the actual crystal structure of *Rb. sphaeroides* by Ermler et al. (1994) the oxygen atom of the acetyl group at D_{M} points away from the Mg^{2+} ion of D_{L}. The basis of the present computations is an earlier version of the crystal structure of *Rb. sphaeroides* (G. Fritzsch and H. Michel, 1994, private communication), in which the acetyl oxygen atom at D_{M} points to the Mg^{2+} ion of D_{L} (denoted as structure **N**). In structure **T** and its analogues the acetyl group at D_{M} is rotated by 180° from structure **N**. After energy minimization of structure **N** using the weak (strong) torsion potential for the acetyl groups, the torsion angle changes from the initial value $\gamma = -133°$ to the value $\gamma = -119°$ (41°) (see Figure 3). The orientation of the acetyl group at D_{M} in the energy-minimized structure **T** deviates by less than 8° from the energy-minimized actual wild-type structure of the RC. Similarly the energy-minimized structure of the wild-type RC with the acetyl group at D_{M} turned by 180° from the orientation in the actual crystal structure deviates from energy minimized structure **N** by less than 8° with respect to the orientation of the acetyl group. This fact justifies the use of the preliminary structures **N** and **T** in the present work. The orientations of the acetyl group at D_{M} differ only slightly

Table 2: Shift of Midpoint Potential ΔE_M (mV) Evaluated with DelPhi[a]

no.	mutant	N_w	T_w	N_s	T_s	expt	$\epsilon_p = \epsilon_m = 2,$ $\epsilon_w = 80$[b]	change in no. of H-bonds
1	FH(M197)[c]	−18	**130**	522	181	125	65	+1
2	HF(L168)	**−129**	−39	−72	−99	−95	−64	−1
3	LH(M160)	**74**	55	54	112	60	36	+1
4	LH(L131)	**85**	94	79	135	80	42	+1
5	FH(M197) + HF(L168)[c]		**34**		15	40	16	+1/−1
6	FH(M197) + LH(M160)[c]		**174**			195	85	+2
7	FH(M197) + LH(L131)[c]		**205**		233	205	101	+2
8	HF(L168) + LH(M160)	**−46**	**−4**			−20	−22	−1/+1
9	HF(L168) + LH(L131)	**−11**	40		34	−20	−5	−1/+1
10	LH(L131) + LH(M160)	**159**	144			130	79	+2
11	FH(M197) + LH(L131) + LH(M160)[c]		**339**			260	166	+3

[a] Bold digits refer to the favored conformation of the acetyl group at D_M (see text). **N** corresponds to a preliminary crystal structure of *Rb. sphaeroides* (Ermler et al., 1994) (see text). In structure **T** the acetyl group at D_M is rotated by 180° as compared with structure **N** before the energy minimization. The subscripts w and s indicate the values of the force constant, 0.5 and 2.0 kcal/mol, respectively, used for the torsion angle potential of the acetyl groups (see eq 2). The reference structure for all calculations is the wild-type structure **N**. The wild-type structure **T** leads to values of the midpoint potential ΔE_M which are shifted by 5 (10) mV to lower values using the w (s) torsion potential for the wild-type and the corresponding mutant structure. The force constant of the acetyl group torsion potential used for the wild-type is the same as that indicated for the mutant structure. [b] These shifts are computed with a dielectric constant of 2 inside and 80 outside of the RC as opposed to $\epsilon_p = 1$ and $\epsilon_m = \epsilon_w = 80$ used for the bulk of the computed shifts of the special pair redox potential. The structures of the RC used for these computations are N_w for the wild-type and the mutant RC except for mutants involving FH(M197) where the mutant structure T_w is used. The computed shifts are half as large as the corresponding computed shifts given in bold face digits in columns N_w and T_w. [c] Before energy minimization of the structures T^0 and T^+ the hydrogen bond geometry found in experiments (Wachtveitl et al., 1993) between the acetyl oxygen atom at D_M and H(M197) is optimized by a reorientation of the histidine ring.
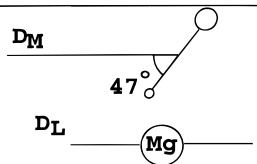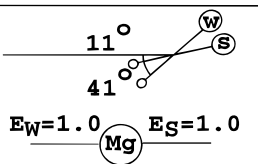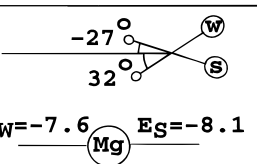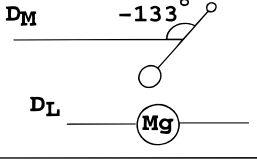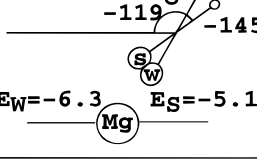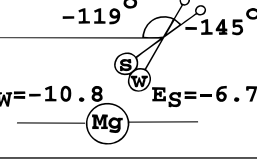

FIGURE 3: Structures of the special pair with different orientations of the acetyl group at D_M. Initial (left) and the corresponding energy-minimized (center) acetyl group orientations of the wild-type structures **N** (preliminary structure: acetyl oxygen atom of D_M bond to Mg^{2+} ion of D_L) and **T** (turned: acetyl group rotated by 180° from the orientation in structure **N**) are depicted schematically. The acetyl group torsion angle defined in the text is given in degrees. The oxygen atoms of the acetyl groups are represented by the larger spheres the methyl groups by the smaller spheres. The letters w and s in the spheres representing the oxygen atoms refer respectively to the weak and strong torsion potential, eq 2. The right part depicts the corresponding acetyl group orientations of the energy-minimized structures of the single point mutation FH(M197) in which a hydrogen bond to the acetyl group of D_M is favored. For more details see text.

if the energy minimization is performed with a positively charged instead of a neutral special pair (see Table 5). The results of the energy minimization of the wild-type and the mutant structure FH(M197) are depicted in Figure 3 for the neutral special pair.

DISCUSSION

Energetic and Hydrogen Bonding of the Ring I Acetyl Group at D_M. In the wild-type structure from *Rb. sphaeroides* the orientation of the acetyl group at D_L is stabilized by the hydrogen bond of the acetyl oxygen atom with H(L168) whereas the acetyl group at D_M has no hydrogen bonding partner. In the actual crystal structure the oxygen atom of the acetyl group at D_M is turned away from the Mg^{2+} ion of D_L (see Figure 2). This acetyl group conformation is only slightly favored by the electron density map. To remove

this uncertainty different orientations of this acetyl group are investigated.

After the energy of the wild-type RC is minimized using the CHARMM force field the orientation of the acetyl group at D_M changes only slightly. With the weak (w) torsion potential, eq 2, the change in the orientation of the acetyl group is larger than with the strong (s) torsion potential. The importance of different conformations of the acetyl group can be judged by comparing the interaction energy of the acetyl group with the protein environment. This energy includes the acetyl torsion potential and all nonbonded energy terms in which the atoms of the acetyl group interact with all other atoms of the considered system. Due to the strong interaction of the acetyl oxygen atom with the Mg^{2+} ion in the wild-type structure **N** the conformational energy decreases by 7.3 kcal/mol (6.1 kcal/mol) for the weak (strong) torsion potential as compared to the conformational energy
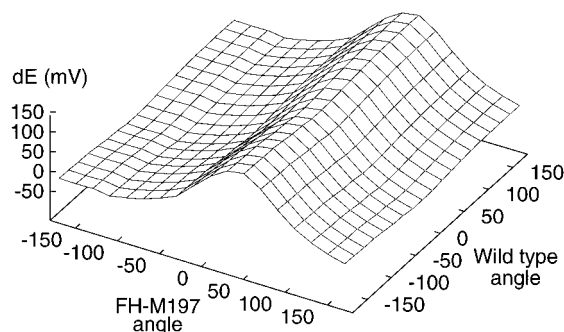
FIGURE 4: Dependence of the shift of E_M of the mutant FH(M197) for different orientations of the acetyl group at D_M. The torsion angle of the acetyl group is set equal for oxidized and reduced RC, which is approximately valid (see Figure 3). Starting from the energy-minimized wild-type structure N^0_w of the reduced RC (for the mutant structure T^0_w), the orientation of the acetyl group at D_M is varied with 10° increment without further energy minimization, yielding an approximate value of the shift only. For the torsion angles 32° and −119° of the acetyl group at D_M corresponding to the energy minima of the wild-type structure N^0_w and the mutant structure T^0_w, respectively, the shift value from this computation is 131 mV.

Table 3: Shift of the E_M of the Mutant FH(M197)[a] Using Different Dielectric Media and Water Content[b]

water content[c]	dielectrics[d] ϵ_p	ϵ_m	ΔE_M (mV)[e]
none	1	1	153
crystal	**1**	**1**	**130**
crystal + overlay	1	1	136
none	1	80	126
crystal	1	80	115
crystal + overlay	1	80	120
crystal/cavities with $\epsilon = 1$[f]	1	80	155
none	4	80	38

[a] Wild-type and mutant FH(M197) have the acetyl group orientation from structure N_w and T_w, respectively (see Table 2). [b] Bold digits refer to the conditions generally used for the computations of electrostatic energies. [c] The water content varies between no water molecules, crystal water molecules only, and crystal and overlay water molecules. [d] Outside of the protein and membrane regime the dielectric constant is $\epsilon_w = 80$ everywhere. In the protein and membrane regime the values of the dielectric constants ϵ_p and ϵ_m are taken as indicated. [e] The experimental value of the shift of the E_M is $\Delta E_M = 125$ mV (Lin et al., 1994b). [f] In the cavities occupied by overlay waters the dielectric constant is set to unity by eliminating the charges of the overlay waters.

of structure **T** (Figure 3). Changing from the reduced to the oxidized state of the special pair a fraction of 0.72 of the unit positive charge is placed on D_L. As a consequence the charge of the Mg^{2+} ion of D_L increases from 0.395 to 0.429. The negative charge of the acetyl oxygen atom at D_M changes only slightly. Hence, the interaction of the acetyl oxygen atom at D_M with the atoms of D_L is stronger for the wild-type structure **N** than for **T**.

In structure **N** the acetyl oxygen atom at D_M can form no hydrogen bond, since it points toward the Mg^{2+} ion of D_L. In structure **T** appropriate for the mutant FH(M197) the acetyl oxygen atom forms a hydrogen bond with H(M197). This bond is quite weak for the strong torsion potential with a hydrogen bond length larger than 3 Å (Table 5). To allow for a stronger hydrogen bonding the weak rather than the strong torsion potential is used. The hydrogen bond in structure **T** leads to a lower value of the interaction energy of the acetyl group with the protein environment. Nevertheless, in structure **N** the interaction energy of the acetyl group

Table 4: Contribution of the Acetyl Groups and Mutated Residues to the Calculated Shift of the E_M (mV)[a]

mutant	acetyl at D_L[b]	acetyl at D_M[b]	mutated residue[c]	other[c]
FH(M197)	4	18	109	21
HF(L168)	−13	3	−98	−31
LH(L160)	11	2	54	20
LH(L131)	−1	6	74	11

[a] The computational conditions are the same as the ones employed for the results in Table 2. The acetyl group orientation at D_M corresponds to the conformations used to obtain the shifts given in bold face digits in Table 2. [b] The acetyl group involves six atoms: the carbon atom, the oxygen atom, and the methyl group bound to the carbon atom. The electrostatic energies needed for the computation of the shifts of E_M are obtained by evaluating the sum in expression 4 only for the atoms of the corresponding acetyl group instead of summing over all atoms of the special pair. The corresponding shift is then calculated by using the expressions 3, 5, and 6. [c] The influence of the mutated residue on the shift of E_M is obtained by evaluating the shift also with vanishing charges for the atoms of the mutated residue. This yields the contribution of the shift from all other residues listed under "other". The discrepancy of this value to the full value of the shift given in Table 2 can then be considered as contribution from the mutated residue, listed under "mutated residue".

Table 5: Energy-Minimized Structures and Energetic of the Mutant FH (M197) for Different Orientations of the Ring I Acetyl Group at D_M[a]

structure[b]	remarks	torsion angle after minimization	E_{pot}[c] (kcal/mol)	H-bond length to His M197[d]
N^0_w	preliminary structure	−119	−10.8	none
N^+_w	weak potential	−118	−17.7	none
T^0_w	preliminary structure 180° rotated	**32**	**−7.6**	**2.29**
T^+_w	weak potential	**26**	**−13.7**	**2.38**
N^0_s	preliminary structure	−145	−6.7	none
N^+_s	strong potential	−142	−15.7	none
T^0_s	preliminary structure 180° rotated	−27	−8.1	3.18
T^+_s	strong potential	−27	−15.4	3.17

[a] Bold digits refer to the favored conformation of the acetyl group at D_M (see text). [b] **N** denotes a preliminary crystal structure which differs from the actual crystal structure with respect to the acetyl group torsion angle. **T** denotes the crystal structure where the ring I acetyl group is rotated by 180° as compared with the structure **N**. For more details see text. The superscripts denote the charge state of the special pair, 0 refers to the reduced and + to the oxidized special pair. The subscripts w (s) refer to a weak (strong) torsion potential at the ring I acetyl groups (see eq 2). [c] Interaction energy between the acetyl group at D_M and its protein environment. [d] Hydrogen bond length between the acetyl oxygen atom at D_M and the nitrogen atom of the hydrogen donor histidine of the mutant H(M197).

is lower due to the bond of the acetyl oxygen atom with the Mg^{2+} ion of D_L. Accordingly in structure N_w the interaction energy of the acetyl group is 3.2 kcal/mol (4.0 kcal/mol) below the interaction energy in structure T_w for the reduced (oxidized) special pair state of the mutant FH(M197) (Table 5). These energy differences for the mutant FH(M197) are less than half of the energy values found for the corresponding wild-type structures. However, due to possible uncertainties in the atomic partial charges these energy differences may not be conclusive to favor one of the structures **N** or **T** for the mutant FH(M197). Such uncertainties are typical for single energy differences as used in the above considerations. Note that for the calculation of ΔE_M double differences of energies are considered (see eq 6). In these double differences many energy terms with uncertain values

may cancel each other. Therefore, the double energy differences from such computations and the corresponding values of the shift of the E_M are more reliable than the values from single energy differences considered above.

Shift of Midpoint Potential E_M. Except for the triple mutant the calculated shifts of the E_M agree approximately with the experimental values in all cases if the dielectric constant in the RC is set to unity $\epsilon_p = 1$ (see bold digits in Table 2). Using $\epsilon_p = 2$ yields values of the shift which are a factor of 2 smaller than with $\epsilon_p = 1$ and consistently smaller than most of the experimental values (Table 2, second column from right). Only results for the wild-type structure **N** are explicitly listed in Table 2. When the wild-type structure **T** is used with the weak (strong) torsion potential, eq 2, for the acetyl groups, the corresponding shifts of the E_M are lower by 5 (10) mV. Hence, the shifts of the E_M calculated with DelPhi can not be used to discriminate between structure **N** and **T** of the wild-type RC. However, there is a preference for the weak torsion potential, which allows the acetyl groups to reorient more easily.

In agreement with the experimental data the calculated midpoint potential E_M *increases* for the single point mutation FH(M197), LH(M160), and LH(L131) in which an additional hydrogen bond is formed with a carbonyl oxygen atom of the special pair by about 74−130 mV. It *decreases* by 85 mV for the single point mutation HF(L168) where a hydrogen bond with the acetyl oxygen atom at D_L is removed. The change in the midpoint potential is small for the double mutants FH(M197) + HF(L168), HF(L168) + LH(M160), and HF(L168) + LH(131) where the number of hydrogen bonds of the carbonyl oxygen atoms of the special pair does not change. The increase of the midpoint potential is about twice as large (159−205 mV) for the double mutants FH(M197) + LH(M160), FH(M197) + LH(131), and LH-(L131) + LH(M160) where the number of hydrogen bonds involving the special pair increases from one to three. The increase of the midpoint potential for mutants, where an additional hydrogen bond forms, is due to the strong Coulomb interaction of the negatively charged oxygen atom of the special pair with the positively charged hydrogen atom. This interaction is very sensitive to small changes in the charge of the special pair oxygen atom which occur if the redox state of the special pair changes. A small selection of relevant atomic partial charges of the different special pair states is given in the Methods section, Computational Conditions for Applications with DelPhi (point 6).

For the double mutants the calculated shifts of the E_M are approximately the sum of the calculated shifts of the single point mutations. The experimental data fulfill this "additivity rule" (Lin et al., 1994a) for the shifts of the E_M even better. Although for the three single point mutations FH(M197), LH(M160), and LH(L131) the calculated shifts of the E_M agree well with the experimental values, the calculated shift disagrees for the corresponding triple mutant. Seemingly, the energy minimization failed for the triple mutant, i.e., the mutant structure with the positively charged special pair was trapped in an unfavorable local energy minimum before reaching a structure which is appropriate for the computation of ΔE_M. The same problem occurred for the mutant FH-(M197) in structure N_s where the calculated shift of the E_M is much too large (see Table 2).

For all computations of the special pair midpoint potential displayed in Tables 2 and 3 the atomic partial charges of the special pair were not adjusted for the different mutants considered, but were taken from the quantum chemical computations of the wild-type structure (Plato et al., 1986, 1991). Recent experiments have shown that for mutants involving a change in the hydrogen bonding pattern of the keto oxygen atoms at the special pair, the asymmetry of the spin density is significantly changed (Rautter et al., 1995). The relevant mutants are LH(M160), LH(L131), and the corresponding double and triple mutants. The charge distribution at the special pair is correlated with the spin density distribution. A change in the asymmetry of the charge distribution should have a noticeable effect on the shift of the special pair redox potential. Although the change of the charge distribution is not taken into account, the computed ΔE_M values of Table 2 agree well with the experimental data.

The mutants involving the point mutation HF(L168) have no hydrogen bond with the acetyl oxygen atom at D_L. These mutants yield calculated shifts of E_M which differ for the mutant structures N_w (the acetyl oxygen atom of D_M points toward the Mg^{2+} ion of D_L) and T_w (the acetyl oxygen atom of D_M points away from the Mg^{2+} ion of D_L). The shifts of E_M calculated for the single point mutation HF(L168) and the double mutant HF(L168) + LH(L131) agree with the experimental data only in structure N_w, where the acetyl oxygen atom of D_M points toward the Mg^{2+} ion of D_L. Assuming that the conformations of the acetyl groups at D_L and D_M are not correlated this would favor the structure N_w also for the wild-type RC. Since the measured shift of E_M is for the double mutant HF(L168) + LH(M160) just between the calculated shifts for the structures N_w and T_w, the structures can not be discriminated on the basis of the computations for this mutant. All other mutants considered here do not allow a clear decision between the structures **N** and **T**.

Influence of the Dielectric Constant on the Shift of E_M. The calculated shift of E_M can depend critically on the values of the dielectric constant used for the solution of Poisson's equation and on the presence or absence of water molecules. The version of DelPhi used here allows to assign different values of the dielectric constant ϵ only in two regimes. According to the considerations in the method section the most reasonable choice is to use the following values of the dielectric constant, $\epsilon_p = \epsilon_m = 1$, in the protein and membrane regime and $\epsilon_w = 80$ outside of the protein and in cavities of the protein large enough and not occupied by water molecules. These values were used to obtain most of the results given in Table 2. Other values of the dielectric constants are also tested. For the most probable hydrogen bonding pattern (bold digits in Table 2) the shift of the E_M is also calculated for $\epsilon_p = \epsilon_m = 2$ and $\epsilon_w = 80$, accounting for polarization effects in the RC (second column from the right in Table 2). Other combinations of values for the dielectric constant are considered for the mutant HF(M197). The calculated shifts of E_M for this mutant are given in Table 3.

Generally, the calculated electrostatic energy differences are smaller for larger values of the dielectric constant. For $\epsilon_p = 2 = \epsilon_m$ and $\epsilon_w = 80$ the calculated values of the shift of the E_M are almost exactly a factor 2 smaller than the ones obtained for $\epsilon_p = 1 = \epsilon_m$ and $\epsilon_w = 80$ (Table 2, last column). This is equivalent to the behavior of a homogeneous dielectric medium where $\epsilon_p = \epsilon_w = \epsilon_m$ and can be expected,

since the special pair in the RC has no direct contact with the solvent and the membrane regime. Accordingly for $\epsilon_p = 4$ the calculated values of the shift of the E_M are about a factor of 4 too small as compared with the corresponding measured values of ΔE_M (see Table 3). An increase of the dielectric constant in the membrane regime to $\epsilon_m = 80$ yields only a small decrease of the calculated shifts of the E_M which is not significant (Table 3).

In the absence of water molecules the calculated shift of the E_M is larger than in the presence of crystal and overlay water molecules. Crystal water molecules seem to screen the electrostatic field more efficiently than a dielectric medium with $\epsilon_w = 80$ used for the protein cavities. Removing the charges of the overlay water molecules but keeping the value of the dielectric constant in the corresponding cavities at unity leads to an increase of ΔE_M from 120 to 155 mV (Table 3). The screening due to overlay water molecules in protein cavities has about the same effect than a dielectric medium with $\epsilon_w = 80$. Therefore, it is justified to remove the overlay water molecules before Poisson's equation is solved.

Influence of the Atomic Partial Charges of the Special Pair on the Shift of E_M. Atomic partial charges for the different redox states of the special pair are not easily available for the mutants considered. Therefore the wild-type special pair charges are also used for the mutants. To check the influence which different special pair charges can have on the calculated shift of the E_M, atomic partial charges used for the mutants have been generated by rescaling the special pair charges of the wild-type RC. The wild-type special pair charge of atom i at BChl monomer D_X is denoted by $q_{X,i}(WT,0)$ [$q_{X,i}(WT,+)$] for the reduced [oxidized] special pair state. For the wild-type RC the total charge at BChl D_X can be expressed as

$$q_X(WT,\alpha) = \sum q_{X,i}(WT,\alpha) \qquad (7)$$

where the sum runs over all special pair atoms and $\alpha = 0,+$ denotes the charge state and $X = L,M$ of the BChl monomer of the special pair. The difference of the atomic partial charges between the two redox states of the special pair can then be expressed by

$$\Delta q_{X,i}(WT) = q_{X,i}(WT,+) - q_{X,i}(WT,0), \quad X = L,M \quad (8)$$

Note that $\Delta q_L(WT) + \Delta q_M(WT) = 1$. Analogous relations hold for the special pair charges in the mutant RC's. The individual differences of atomic partial charges of the mutant RC's are obtained by scaling the corresponding differences of the wild-type special pair charges averaged over equivalent atoms of the D_L and D_M BChl monomers as follows:

$$\Delta q_{X,i}(\text{mut}) = (\Delta q_{L,i}(WT) +$$

$$\Delta q_{M,i}(WT))\frac{\Delta q_X(\text{mut})}{\Delta q_L(\text{mut}) + \Delta q_M(\text{mut})} \quad (9)$$

The charges of the reduced (neutral) special pair are assumed to be the same for the wild-type and mutant RC, $q_{X,i}(\text{mut},0) = q_{X,i}(WT,0)$, whereas the charges of the oxidized special pair in the mutant RC are calculated as $q_{X,i}(\text{mut},+) = q_{X,i}(WT,0) + \Delta q_{X,i}(\text{mut})$, where $\Delta q_{X,i}(\text{mut})$ is evaluated from expression 9.

For the single point mutations LH(L131) and LH(M160) which add a hydrogen bond to the keto oxygen atom of D_L and D_M, respectively, the asymmetry of the spin density differs considerably form the wild-type RC (Rautter et al., 1995). Assuming that the asymmetry of the spin density is identical to the asymmetry of the charge distribution in the oxidized (positively charged) special pair state, one has in units of the elementary charge $\Delta q_L(LH(L131)) = 0.47$, $\Delta q_M(LH(L131)) = 0.53$, and $\Delta q_L(LH(M160)) = 0.83$, $\Delta q_M(LH(M160)) = 0.17$, as compared to $\Delta q_L(WT) = 0.67$ and $\Delta q_M(WT) = 0.23$ derived from the spin densities of the wild-type RC (Rautter et al., 1995).

With these charges for the special pair atoms the mutant RC's were energy minimized and the shifts of the E_M were calculated with DelPhi using the energy-minimized structures. With a dielectric constant of unity in the RC ($\epsilon_p = 1$) one obtains $\Delta E_M(LH(L131)) = -4$ mV and $\Delta E_M(LH(M160)) = 121$ mV as compared to the experimental values of 60 and 80 mV, respectively. For a larger dielectric constant in the RC of $\epsilon_p = 2$ the corresponding values of the shift are -2 and 60 mV, almost exactly half as large as for $\epsilon_p = 1$. Since for the majority of the other mutants no agreement could be obtained for $\epsilon_p = 2$, the agreement with the experimental value of the shift obtained for the mutant LH(M160) must be considered to be fortuitous. Obviously the special pair charges can have a large influence on the calculated shift of the E_M. The lack of success using the scaled charges derived from the special pair charges of the wild-type RC is probably due to the charges which are not adequate. Another possibility is that the structures used for the computations of ΔE_M are inappropriate. It is astonishing that by using the wild-type special pair charges also for the mutants LH(L131) and LH(M160) the calculated shifts of the E_M agree with the experimental values (see Table 2). To clarify this point proper atomic partial charges of the special pair which account also for the protein environment must be used in future computations of the shift of E_M.

Dependence of ΔE_M on the Mutated Residue and on the Orientation of the Acetyl Group at D_M. The direct contributions of the acetyl groups to the calculated shift of the E_M can be obtained by extending the sum of the products of the special pair charges $q_i(\alpha)$ and the electrostatic potential at the corresponding special pair atoms $\Phi_i(\alpha)$, eq 4, over the acetyl group atoms only. These contributions are generally small for both acetyl groups (at D_L and D_M). This can be inferred from Table 4, where results for all single point mutations considered in this study are given. To obtain the contributions of the mutated residues separate computations are required. The electrostatic potential at the special pair atoms $\Phi_i(\alpha)$ can be evaluated with vanishing atomic partial charges of the mutated residue for the mutant as well as the wild-type RC. The shifts of the E_M computed with these electrostatic potentials contain the influence of the special pair environment except the mutated residue. These values are small but not always negligible (Table 4, last column). The major contribution is the complement of this partial shift to the corresponding full value of the shift displayed in Table 2 with bold face digits. It is the contribution of the mutated residue.

In Figure 4 the dependence of the shift of the special pair redox potential on the orientation of the acetyl group at D_M is shown for the mutant FH(M197) using the weak torsion potential, eq 2. The torsion angles are varied in the wild-

type and the mutant RC. To obtain the landscape of ΔE_M, displayed in Figure 4, it is assumed that the torsion angles are equal in the reduced and oxidized special pair state. This is approximately valid for the energy minimized structures as can be seen from Figure 3. The computations of the shift of E_M are based on the energy-minimized structures of RC's in the reduced state. These are the structure $\mathbf{N}_w$ for the wild-type RC and the structure $\mathbf{T}_w$ for the mutant RC. Starting from these structures the acetyl group at D_M is rotated in increments of 10° without further energy minimization. Hence, the shifts of E_M displayed in Figure 4 can be related only qualitatively with the calculated values of ΔE_M given in Table 2. Nevertheless, for the mutant FH(M197) the value of $\Delta E_M = 130$ mV from Table 2 is identical to the value of 131 mV obtained from Figure 4 for the same acetyl group orientations.

Since energy terms involving the acetyl groups contribute only a small portion to the exact value of the calculated shift of the E_M (see Table 4 and the discussion above), one may argue that different orientations of the acetyl groups may have little influence on the calculated value of the shift of E_M. Figure 4 demonstrates that this is not the case. Obviously the electrostatic interaction of the mutated residue can vary strongly with the orientation of the acetyl group at D_M. This is exemplified for the mutant FH(M197), where one observes a strong dependence of the shift of E_M on the orientation of the acetyl group in the mutant RC. The maximum value of the shift of E_M (131 mV) is reached if the acetyl group oxygen atom forms a hydrogen bond with the histidine of residue M197. The dependence on the corresponding torsion angle in the wild-type RC is small. This is corroborated by the small differences in the shift of E_M obtained by using the structures $\mathbf{T}$ and $\mathbf{N}$ for the wild-type RC. The corresponding values of ΔE_M are 5 mV for the weak and 10 mV for the strong torsion potential.

By varying the acetyl group orientation at D_M in the wild-type RC, the bond between the Mg^{2+} ion at D_L and the acetyl oxygen atom can be turned on and off. In the mutant FH-(M197) RC a hydrogen bond between the acetyl oxygen atom and His M197 can also be turned on and off. Only if hydrogen bond is turned on and off is a strong dependence of ΔE_M on the acetyl group orientation observed. The bond with the Mg^{2+} ion at D_L seems not to contribute to the value of ΔE_M. This is due to the specific variation of the atomic partial charges at the Mg^{2+} ion and the acetyl oxygen atom which occurs, when the special pair redox state changes. The positive charge at the Mg^{2+} ion increases and the negative charge at the acetyl oxygen atom decreases by changing from the reduced to the oxidized special pair state. Since the relevant Coulomb interaction influencing ΔE_M contains the product of these charges, the net effect of the changes in the atomic partial charges cancels approximately. This can explain the insensitivity of ΔE_M on the acetyl group orientation in the wild-type RC.

Problems with the Computation of ΔE_M. The evaluation of electrostatic energies by solving Poisson's equation for suitably energy-minimized structures is a relatively fast method to calculate shifts of the redox potential E_M. If reasonable three-dimensional structures are obtained by energy minimization, then one can expect that the method yields reliable results. Sometimes the local minimum reached by the energy minimization is too far away from the global minimum to yield an appropriate structure. This

is demonstrated by the triple mutant where the directly calculated shift of the E_M differs from the experimental value by 80 mV, whereas the sum of the calculated shifts from the three single point mutations deviates by less than 25 mV.

A second example is the mutant FH(M197), where for the wild-type and mutant RC in structure $\mathbf{N}_s$ the calculated shift is by far too large (Table 2). Although the structure $\mathbf{N}_s$ is in principle inappropriate for this mutant, this fact is not sufficient to explain such a large discrepancy.

For the single point mutation FH(M197) in structure $\mathbf{T}$ another problem of inappropriate structures becomes evident by directly comparing the acetyl group conformation at D_M for the strong and weak torsion potentials (see Figure 3, right, and Table 5). During energy minimization the acetyl group at D_M moves to a new orientation for the strong torsion potential, whereas for the weak torsion potential the acetyl group orientation does not change considerably from its initial orientation (see Figure 3). The absolute value of the torsion angle after energy minimization is about the same for the weak and strong torsion potential, so that the torsion energy of the acetyl group alone assumes a higher value in structure $\mathbf{T}_s$ than in structure $\mathbf{T}_w$. Nevertheless, the total interaction energy of the acetyl group is lower for the energy-minimized structure $\mathbf{T}_s$ than for $\mathbf{T}_w$. From this it becomes evident that by accidental sterical hindrance in structure $\mathbf{T}_w$ the acetyl group is unable to reorient during energy minimization to reach the energetically more favorable acetyl group orientation obtained in structure $\mathbf{T}_s$. From this point of view the agreement with the experimental ΔE_M value of mutant FH(M197) using structure $\mathbf{T}_w$ may be fortuitous.

In all of these cases the problem is related to insufficient structural relaxation by using energy minimization. This can in principle be avoided by using simulated annealing instead of energy minimization. (For the conditions of simulated annealing see point 5 in the Methods section.) However, the shifts of the E_M calculated with structures obtained by simulated annealing differ considerably from the experimental data. (No explicit data are shown.) This may be due to structural defects which are generated during the heating of the RC to a temperature of 400 K. Hence, the suitability of a three-dimensional structure for the calculation for electrostatic energies cannot be estimated from its energy value alone.

CONCLUSIONS

The shifts of the E_M of the special pair of the RC *Rb. sphaeroides* have been calculated for eleven different mutants by solving Poisson's equation for energy-minimized structures of the RC. In these mutants the hydrogen bonding pattern of the special pair is varied. The number and strength of those hydrogen bonds change the redox potential of the special pair, which determines the driving force of the functionally important electron transfer processes. Hence, the computational reproduction of the special pair redox potentials of different mutants helps to understand how the protein environment tunes this potential. In this context the reorientation of the acetyl groups at the special pair may serve as a switch which adjusts the redox potential of the special pair. Therefore, the influence of the orientation of the acetyl groups on the calculated value of the midpoint potential was investigated in more detail.

In ten out of eleven cases good agreement with the experimental values was obtained. As for the experimental

data the calculated shifts of double mutants could also be obtained by adding the calculated shifts from the corresponding single point mutations. A better agreement with the experimental shifts of the E_M was reached if the torsion potential of the acetyl groups at the special pair was assumed to be relatively weak to allow for a large reorientation of the acetyl groups.

The special pair is well isolated from the solvent and membrane regime such that the calculated shifts of the E_M depend mainly on the value of the dielectric constant ϵ_p used for the RC. In contrast to earlier applications solving Poisson's equation, good agreement with measured data is obtained for $\epsilon_p = 1$, whereas the calculated shifts are consistently too small, if the value of the dielectric constant used for the RC is larger ($\epsilon_p \geq 2$). Explicit water molecules placed in the protein cavities screen the dielectric interactions equivalently to a dielectric medium with the dielectric constant $\epsilon = 80$.

For two mutants, HF(L168) and HF(L168) + LH(L131), the calculated shifts of the E_M agree with the experimental values only if the acetyl oxygen atom at D_M points toward the Mg^{2+} ion of D_L. In the other cases no change of the orientation of the acetyl group at D_M was necessary. The computations of the interaction energy of the acetyl group at D_M with the protein environment also favor a wild-type structure, where the oxygen atom of the acetyl group is bonded to the Mg^{2+} ion of D_L. On the other hand in the crystal structure there is a weak preference for the oxygen atom to point away from the Mg^{2+} ion and the atoms of the acetyl group have nearly an in-plane orientation with respect to the porphyrin plane.

A major uncertainty of the present computations are the values of the atomic partial charges of the special pair. In the present treatment these are neither adjusted to the different orientations of the acetyl group nor are the charges computed quantum chemically for the different mutant RC's and their special pair environment. A simple rescaling of the special pair charges on the basis of the quantum chemically computed special pair charges of the wild-type RC and the measured asymmetry of the spin density of the special pair (Rautter et al., 1995) did not succeed. In the future atomic partial charges based on detailed quantum chemical calculations must be used. Those are rather elaborate computations. With the exception of the mutants involving LH(L131) or LH(M160), they are, however, not expected to basically change the results obtained in this paper.

REFERENCES

Allen, J. P., Feher, G., Yeates, T. O., Komiya, H., & Rees, D. C. (1987) *Proc. Natl. Acad. Sci. U.S.A. 84*, 6162−6166.

Bixon, M., Jortner, J., & Michel-Beyerle, M. E. (1991) *Biochim. Biophys. Acta 1056*, 301−315.

Bixon, M., Jortner, J., & Michel-Beyerle, M. E. (1992) in *The Photosynthetic Bacterial Reaction Center: II. Structure, Spectroscopy and Dynamics* (Breton, J., & Verméglio, A., Eds.) pp 291−300, Plenum Press, New York.

Blumhagen, K., Muegge, I., & Knapp, E. W. (1995) *Int. J. Quantum Chem.* (in press).

Breton, J., Martin, J. L., Fleming, G. R., & Lambry, J. C. (1988) *Biochemistry 27*, 8276−8284.

Brooks, B. R., Bruccoleri, R. E., Olafson, B. D., States, D. J., Swaminathan, S., & Karplus, M. (1983) *J. Comput. Chem. 4*, 187−217.

Chang, C.-H., Tiede, D., Tang, J., Smith, U., Norris, J., & Schiffer, M. (1986) *FEBS Lett. 205*, 82−86.

Chirino, A. J., Lous, E., J., Huber, M., Allen, J. P., Schenck, C. C., Paddock, M. L., Feher, G., & Rees, D. C. (1994) *Biochemistry 33*, 4584−4593.

Coulson, C. A., & Eisenberg, D. (1966) *Proc. R. Soc. (London) A291*, 445−451.

Creighton, S., Hwang, J.-K., Warshel, A., Parson, W. W., & Norris, J. (1988) *Biochemistry 27*, 774−781.

Churg, A. K., & Warshel, A. (1986) *Biochemistry 25*, 1675−1681.

Deisenhofer, J., Epp, O., Miki, K., Huber, R., & Michel, H. (1985) *Nature 318*, 618−624.

Deisenhofer, J., & Michel, H. (1991) *Annu. Rev. Biophys. Chem. 20*, 247−260.

Dewar, M. J. S., Hashmall, J. A., & Venier, C. G. (1968) *J. Am. Chem. Soc. 90*, 1953−1963.

Elber, R., & Karplus, M. (1990) *J. Am. Chem. Soc. 112*, 9161−9175.

Ermler, U., Fritzsch, G., Buchanan, S. K., & Michel, H. (1994) *Structure 2*, 925−936.

Farchaus, J. W., Wachtveitl, J., Mathis, P., & Oesterhelt, D. (1993) *Biochemistry 32*, 10885−10893.

Frisch, M. J., Trucks, G. W., Head-Gordon, M., Gill, P. M. W., Wong, M. W., Foresman, J. B., Johnson, B. G., Schlegel, H. B., Robb, M. A., Replogle, E. S., Gomperts, R., Andres, J. L., Raghavachari, K., Binkley, J. S., Gonzales, C., Martin, R. L., Fox, D. J., Defrees, D. J., Baker, J., Stewart, J. J. P., & Pole, J. A. (1992) *Gaussian 92*, Revision C, Gaussian Inc., Pittsburgh, PA.

Gilson, M. K., & Honig, B. (1988) *Proteins 4*, 7−18.

Gilson, M. K., Rashin, A., Fine, R., & Honig, B. (1985) *J. Mol. Biol. 183*, 503−516.

Gilson, M. K., Sharp, K. A., & Honig, B. (1987) *J. Comput. Chem. 9*, 327−335.

Gunner, M. R., & Honig, B. (1991) *Proc. Natl. Acad. Sci. U.S.A. 88*, 9151−9155.

Hoff, A. J. (1988) in *The Photosynthetic Bacterial Reaction Center: Structure and Dynamics* (Breton, Y., & Verméglio, A., Eds.) pp 98−99, Plenum Press, New York.

Jorgensen, W. L., Chendrasekar, J., Madura, J. D., Impley, R. W., & Klein, M. L. (1983) *J. Chem. Phys. 79*, 926−935.

Kirkpatrick, S., Gelatt, C. D., & Vecchi, M. P. (1983) *Science 220*, 671−680.

Kirmaier, C., & Holten, D. (1987) *Photosynth. Res. 13*, 225−260.

Kirmaier, C., & Holten, D. (1993) in *The Photosynthetic Reaction Center* (Deisenhofer, J., & Norris, J. R., Eds.) Vol. 2, pp 49−70, Academic Press, San Diego, CA.

Klapper, I., Hagstrom, R., Fine, R., Sharp, K., & Honig, B. (1986) *Proteins 1*, 47−59.

Knapp, E. W., & Nilsson, L. (1990) in *Reaction Centers of Photosynthetic Bacteria* (Michel-Beyerle, M. E., Ed.) pp 437−450, Springer, New York.

Lendzian, F., Huber, M., Isaacson, R. A., Endeward, B., Bönigk, B., Möbiusm, K., Lubitz, W., & Feher, G. (1993) *Biochim. Biophys. Acta 1183*, 139−160.

Lin, X., Murchison, H. A., Nagarijan, V., Parson, W. W., Allen, J. P., & Williams, J. C. (1994a) *Proc. Natl. Acad. Sci. U.S.A. 91*, 10265−10269.

Lin, X., Williams, J. C., Allen, J. P., & Mathis, P. (1994b) *Biochemistry 33*, 13517−13523.

Mattioli, T. A., Williams, J. C., Allen, J. P., & Robert, B. (1994) *Biochemistry 33*, 1636−1643.

Mattioli, T. A., Lin, X., Allen, J. P., & Williams, J. C. (1995) *Biochemistry 34*, 6142−6152.

Michel, H., Epp, O., & Deisenhofer, J. (1986) *EMBO J. 5*, 2445−2452.

Mulliken, R. S. (1955) *J. Chem. Phys. 23*, 1833−1840.

Murchison, H. A., Alden, R. G., Allen, J. P., Pelequin, J. M., Taguchi, A. K. W., Woodbury, N. W., & Williams, J. C. (1993) *Biochemistry 32*, 3498−3505.

Nabedryk, E., Allen, J. P., Taguchi, A. K. W., Williams, J. C., Woodbury, N. W., & Breton, J. (1993) *Biochemistry 32*, 13879−13885.

Nagarajan, V., Parson, W. W., Davis, D., & Schenck, C. C. (1993) *Biochemistry 32*, 12324−12336.

Nicholls, A., & Honig, B. (1991) *J. Comput. Chem. 12*, 435−445.

Parson, W. W., & Warshel, A. (1987) *J. Am. Chem. Soc. 109*, 6152−6163.

Plato, M., Tränkle, E., Lubitz, W., Lendzian, F., & Möbius, K. (1986) *Chem. Phys. 107*, 185−196.

Plato, M., Möbius, K., & Lubitz, W. (1991) in *Chlorophylls* (Scheer, H., Ed.) pp 1015−1046, CRC Press, Boca Raton, FL.

Pople, J. A., & Beveridge, D. L. (1970) *Approximate Molecular Orbital Theory*, McGraw-Hill, New York.

Rautter, J., Lendzian, F., Schulz, C., Fetsch, A., Kuhn, M., Lin, X., Williams, J. C., Allen, J. P., & Lubitz, W. (1995) *Biochemistry 34*, 8130−8143.

Scherer, P. O. J., & Fischer, S. F. (1989a) *J. Phys. Chem. 93*, 1633−1637.

Scherer, P. O. J., & Fischer, S. F. (1989b) *Chem. Phys. 131*, 115−127.

Wachtveitl, J., Farchaus, J. W., Das, R., Lutz, M., Robert, B., & Mattioli, T. A. (1993) *Biochemistry 32*, 12875−12886.

Wade, R. C., Mazor, M. H., McCammon, J. A., & Quiocho, F. A. (1991) *Biopolymers 31*, 919−931.

Warshel, A., & Parson, W. W. (1987) *J. Am. Chem. Soc. 109*, 6143−6151.

Williams, J. C., Alden, R. G., Murchison, H. A., Peloquin, J. M., Woodbury, N. W., & Allen, J. P. (1992) *Biochemistry 31*, 11029−11037.

Woodbury, N. W., Becker, M., Middendorf, D., & Parson, W. W. (1985) *Biochemistry 24*, 7516−7521.

Yeates, T. O., Komiva, H., Chirino, A., Rees, D. C., Allen, J. P., & Feher, G. (1988) *Proc. Natl. Acad. Sci. U.S.A. 85*, 8487−8491.

Zinth, W., & Kaiser, W. (1993) in *The Photosynthetic Reaction Center* (Deisenhofer, J., & Norris, J. R., Eds.) Vol. 2, pp 71−88, Academic Press, San Diego, CA.